SOLAR ARRAY IN SIMULATED LEO PLASMA ENVIRONMENT

Boris Vayner
Ohio Aerospace Institute, NASA Glenn Research Center
MS 302-1, 21000 Brookpark Road
Cleveland, OH 44135
Phone: (216)-433-8058
Fax: (216)-433-6106
E-mail: vayner@grc.nasa.gov

Joel Galofaro
Dale Ferguson
NASA Glenn Research Center

Abstract

Six different types of solar arrays have been tested in large vacuum chambers. The low Earth orbit plasma environment was simulated in plasma vacuum chambers, where the parameters could be controlled precisely. Diagnostic equipment included spherical Langmuir probes, mass spectrometer, low-noise CCD camera with optical spectrometer, video camera, very sensitive current probe to measure arc current, and a voltage probe to register variations in a conductor potential. All data (except video) were obtained in digital form that allowed us to study the correlation between external parameters (plasma density, additional capacitance, bias voltage, etc) and arc characteristics (arc rate, arc current pulse width and amplitude, gas species partial pressures, and intensities of spectral lines). Arc inception voltages, arc rates, and current collections are measured for samples with different coverglass materials and thickness, interconnect designs, and cell sizes. It is shown that the array with wrapthrough interconnects have the highest arc threshold and the lowest current collection. Coverglass design with overhang results in decrease of current collection and increase of arc threshold. Doubling coverglass thickness causes the increase in arc inception voltage. Both arc inception voltage and current collection increase significantly with increasing a sample temperature to 80 C. Sustained discharges are initiated between adjacent cells with potential differences of 40 V for the sample with 300 μm coverglass thickness and 60 V for the sample with 150 μm coverglass thickness. Installation of cryogenic pump in large vacuum chamber provided the possibility of considerable outgassing of array surfaces which resulted in significant decrease of arc rate. Arc sites were determined by employing a video-camera, and it is shown that the most probable sites for arc inception are triple-junctions, even though some arcs were initiated in gaps between cells. It is also shown that the arc rate increases with increasing of ion collection current. The analysis of optical spectra (240-800 nm) reveals intensive narrow atomic lines (Ag, H) and wide molecular bands (OH, CH, SiH, SiN) that confirms a complicated mechanism of arc plasma generation. The results obtained seem to be important for the understanding of the arc inception mechanism, which is absolutely essential for progress toward the design of high-voltage solar array for space application.

Introduction

The purpose of the current paper is to test a possibility of significant increase of arc thresholds by modifications of conventionally designed solar arrays. Previous studies of arc inception mechanism [1-4] suggest that such modifications can be done in the following directions: I) to insulate conductor-dielectric junction from a plasma environment (wrapthrough interconnects); II) to change a coverglass geometry (overhang); III) to increase a coverglass thickness; IV) to outgas areas of conductor-dielectric junctions, V) to use coverglass with lower dielectric permittivity and higher conductivity. The operation of high-voltage array in LEO produces also the parasitic current power drain on the electrical system. Moreover, the current collected from space plasma by solar arrays determines the spacecraft floating potential that is very important for the design of spacecraft and its scientific apparatus. In order to verify the validity of suggested modifications and to measure current collection six different solar array samples have been tested in large vacuum chamber. Five samples (36 silicon based cells) consist of three strings in each sample containing 12 cells connected in series. One sample contains nine cells (2x4 cm) arranged in three strings, and this sample is used for measuring arc plasma optical spectra. Thus, arc rate and current collection can be measured on every string independently, or on a whole sample when strings are connected in parallel. The heater installed in the chamber provides the possibility to test samples under temperature as high as 80 C that simulates the LEO operational temperature. The experimental setup is described below.

Experimental Setup

Low Earth Orbit (LEO) plasma environment was simulated in two different vacuum vessels: 1) horizontal vacuum chamber (1.8 m diameter and 2 m long) equipped with cryogenic pump; 2) large vacuum tank (2.2 m diameter and 3 m height) with four diffusion pumps. The vacuum equipment provided pressure as low as 0.5 μTorr. The essential difference between these two tanks is that the residual water vapor partial pressure in horizontal chamber is five times lower than in vertical tank. Each vessel has one Kaufman plasma source that generates xenon plasma with electron density $n_e=(0.1\text{-}10)\cdot 10^5$ cm^{-3} , temperature T_e=0.6-1.2 eV, and neutral gas pressure $p=(0.7\text{-}7)\cdot 10^{-5}$ Torr which can be kept steady during the experiment. To measure plasma parameters, Langmuir probes with diameter 2 cm were employed (two in each tank). To determine an ion distribution function and to improve measurements of electron temperature one retarding potential analyzer (RPA) was mounted on the bottom of vertical tank. It was found that the ion (xenon) thermal flux in the experiment is about three times lower than ram ion flux in LEO, and the electron temperature is 5-10 times higher than in ionosphere. However, the number densities are simulated with a quite high accuracy, and one can believe that the results of high-voltage experiments in vacuum chambers are fairly adequate to the outcomes of processes in LEO plasma. To control plasma chemical composition (particularly, water vapor and oil partial pressures) a quadruple mass spectrometer was installed in each tank.

The sample (or set of samples) is vertically mounted in the middle of the chamber, and it is biased to a voltage power supply through a capacitor and a 10 kΩ resistor network back to ground. An additional power supply (Solar Array Simulator-SAS) is used to generate electrical field perpendicular to the dielectric side surface for investigating arc inception on semiconductor-dielectric junction and inception of sustained discharges between adjacent strings. Diagnostic

equipment includes two current probes to measure discharge current and SAS current, and one voltage probe that allows us to register voltage pulse on the sample during the discharge. To measure optical spectra of arc plasma an intensified CCD (1024x512 pixel) camera with optical spectrometer is installed. The arc sites are determined by employing a video camera and VCR. Most experiments were performed at room temperature (15C), but some tests had been done at the temperature +80 C simulating the exposure of solar array to full sun in LEO.

Arc Spectra

Previous experimental data and theoretical analysis have demonstrated that water molecules adsorbed on the side surface of dielectric (coverglass+adhesive) can play a decisive role in the process of arc inception [5-7]. It is known that spectra of vacuum arcs consist of cathode metal lines only [8] but adding air in vacuum chamber (10^{-4} Torr) results in appearance of hydrogen and hydroxyl lines [9]. Partial pressure of water vapor and nitrogen is always below 10^{-5} Torr for the current experiment. Thus, the presence of hydrogen and hydroxyl in the arc plasma would be a good indicator of water ions dissociative recombination. The presence of other species in arc plasma may reveal other important processes in the discharge development. To elucidate all these problems the measurements of optical spectra have been performed for silicon solar array sample (nine cells). All dielectric-conductor junctions besides one interconnect area were insulated by tape to exclude spectra from arcs between cells. The spectral resolution was determined as 0.12 nm/pixel by using standard calibration lamps. To increase the arc luminosity an additional capacitor (usually 1 μF) was installed between negatively biased electrode and ground. Gate pulse generator provided varying both gate pulse width and time delay; thus, it was possible to measure the intensities of spectral lines on different stages of a discharge development. In addition to hydrogen (H_α), hydroxyl (OH), and metal lines (Ag) arcing on the sample revealed also some molecular radicals identified according to Ref. 10 (Fig.1).

The results of spectral measurements, observation of decreasing arc rate with number of arcs (conditioning), and theoretical estimates [11] are very strong argument in favor of the idea that in order to raise arc threshold solar array surfaces must be thoroughly outgassed. The validity of this hypothesis has been confirmed by ground tests described in Sec. 5 below.

Outgassing of Solar Array Samples

When spacecraft is coming out of eclipse, solar array temperature is rising due to exposure to Sun radiation. Operational temperature of an array in LEO conditions is approximately 80-100 C. It is believed that the adsorbed contaminants from the array surface are evaporating at a high rate due to heating. On another hand, when solar array sample is installed in a vacuum chamber its surface is contaminated not only by "natural" species (adsorbed water, atmospheric gases, and products of a technological process) but also other contaminants. The most abundant of these contaminants is vacuum pump oil. To measure chemical composition of background vacuum and to determine plasma contamination due to heating, the quadruple mass-spectrometers are installed in both large chambers. Two solar array samples are mounted on an aluminum sheet with electrical heater placed on the back (Fig.2). This heater provides enough power to radiantly heat sample from 15 C to 80 C for about 50 minutes (Fig.3). It is seen that the increase in water

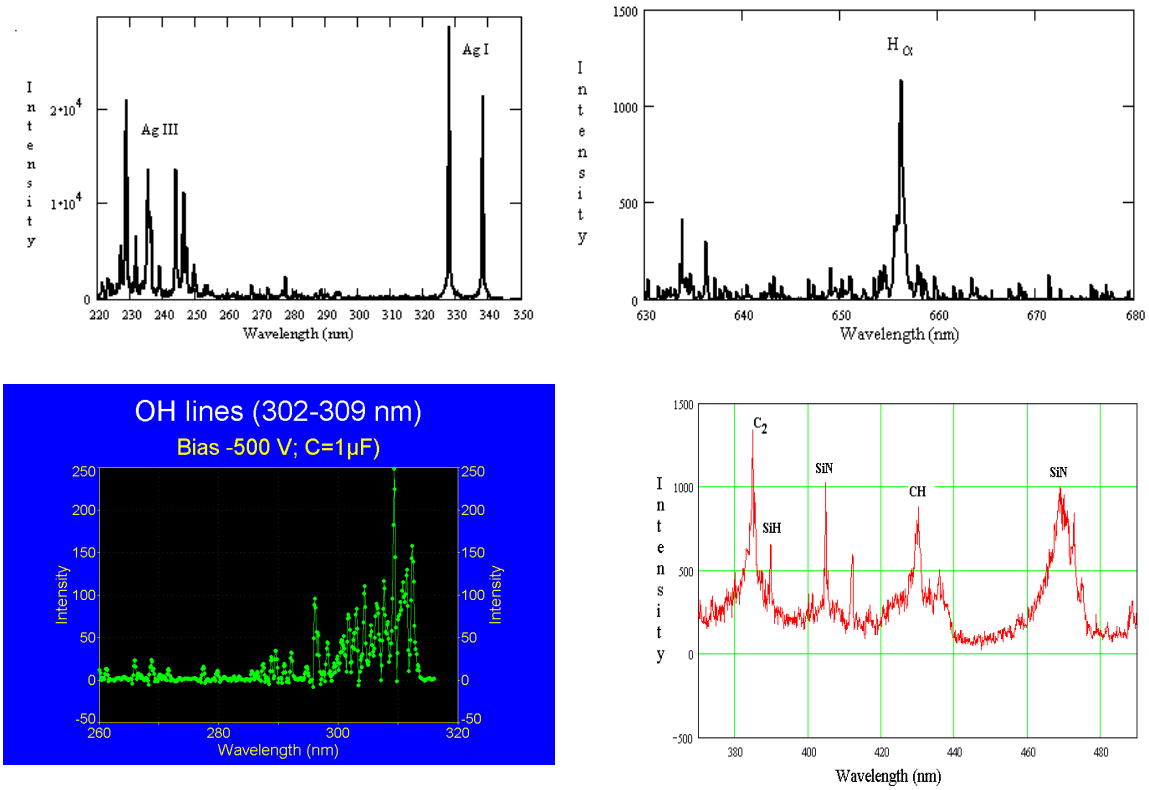

Figure 1. One example of emission spectrum of arc plasma.

vapor partial pressure is considerably higher than the plain isochoric increase $\frac{\Delta p}{p_0} = \frac{\Delta T}{T_0}$,and this observation confirms the presence of water adsorbed on solar array surface.

Five cycles of heating-cooling sample in vacuum chamber resulted in significant drop of residual water vapor pressure (Fig.4).

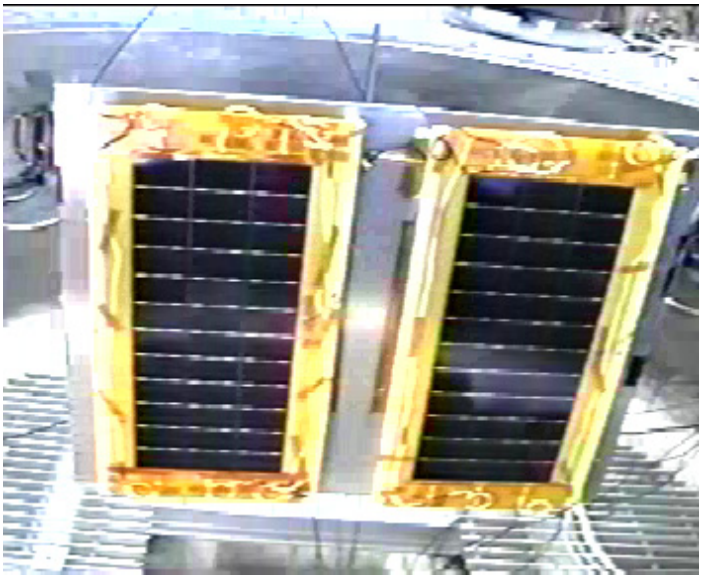

Figure 2. Solar array samples installed in vacuum chamber.

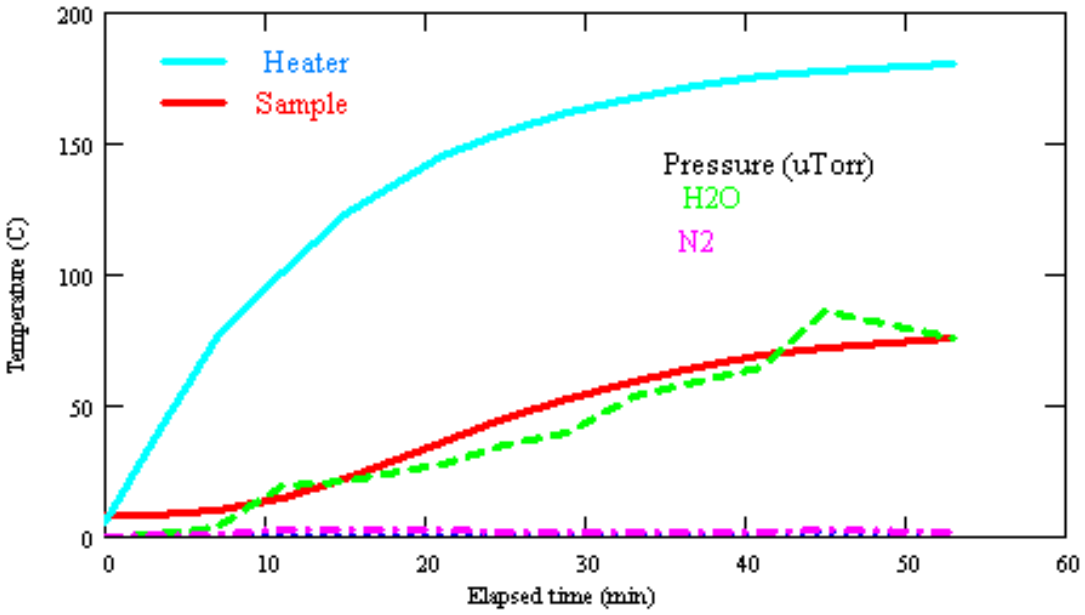

Figure 3. Increase of water vapor pressure is considerably higher than plain isochoric increase.

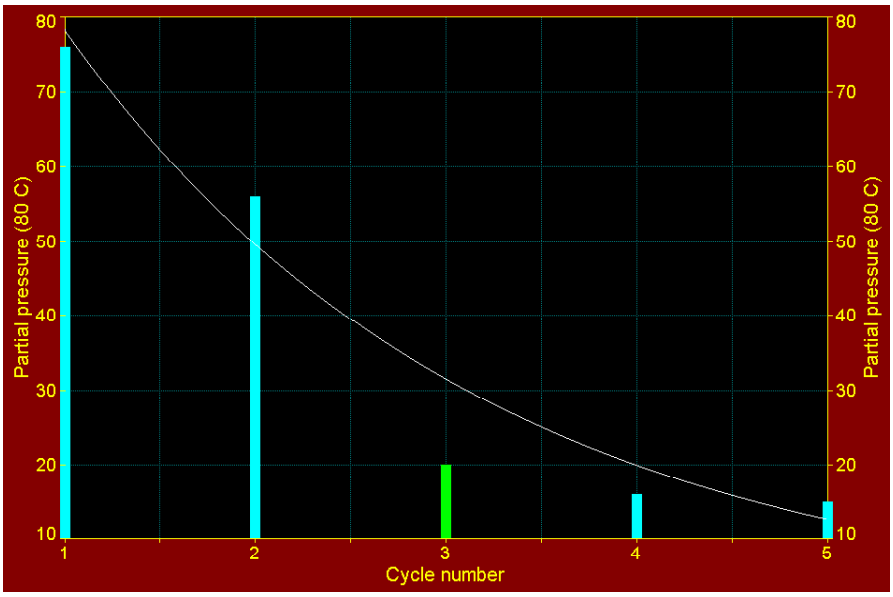

Figure 4. Water vapor partial pressure in course of thermal cycling (rel. units).

Arcing in Plasma

Five types of tested solar arrays are shown in Table 1. Each string (12 cells in series) is tested separately to measure arc inception voltage and arc rate. Measurements reveal significant differences in these parameters even for strings belonging to one sample. There are two reasons explaining such observations: manufacturing process peculiarities and geometrical design of a sample. In fact, the middle string is separated from neighboring strings by narrow gaps (0.8 mm) covered with a thin RTV layer while two other strings have edges with underlying semiconductor and dielectric exposed to the plasma. Manufacturing peculiarities demonstrate themselves when one compares arc parameters for two outer strings and finds considerable differences. And arc sites are located mostly on interconnects for middle string while great part of arcs on outer strings has been observed on cell edges. To preserve the homogeneity of collected data one common experimental procedure is used for all measurements of arc inception voltages and arc rates: 1) string is initially biased to voltage well below an expected arcing threshold; 2) 15-30 minute time interval is allowed to register (or to not register) an arc; 3) voltage is increased on 10-20 V; 4) arc rate is defined as an average over a respective time span. On the first stage of the test, two samples (#1 and #2 in Table 1) are mounted on the heater plate and installed in chamber. The results of measurements for middle strings at the room temperature are shown in Fig.5. Obviously, arc inception voltage is lower for the panel with thinner coverglass, and arc rates differ significantly. Arc rates have been also determined at high temperature (Fig.6).

Arc rates are widely scattered over a range of voltages 280-380 V. In general, the temperature rise to 80 C results in significant increase of arc inception voltage (40-60 V). In particular, inner strings are not arcing below 300 V. It is worth noting that measurements shown above have been done at comparatively high water vapor partial pressures: 4 μTorr at 15 and 15-30 μTorr at 80 C. These values are much higher than one can anticipate in LEO conditions. The

Table 1. Five types of solar array samples tested in the large chambers.

Sample No	Coverglass Thickness (μm)	Material	Overhang (μm)	Cell size (cm)	Interconnect
1	300	UVR	0	4x6	exposed
2	150	UVR	0	4x6	exposed
3	150	CMX UVR	0	4x6	exposed
4	150	UVR	250	4x6	exposed
5	150	UVR	0	8x8	wrapthrough

decrease of an arc rate during the process of continuing arcing (conditioning) has been measured by biasing the whole sample #2 to -400 V and measuring average arc rate for every four minutes. Additional capacitance is increased from 0.22 μF to 1μF to accelerate conditioning. After about 70 arcs, arc rate drops from 3.25 arc/min to the magnitude of 1 arc/min and stays practically steady for the next 30 arcs. To verify the influence of plasma density on arc rate this parameter has been increased by factor 1.5, and arc rate was measured for the next 100 arcs. Finally, arc rate has decreased to 0.25 arc/min after about 200 arcs. Thus, the influence of conditioning on previous measurements of arc rates for separate strings belonging to different samples is insignificant, particularly because of low capacitance (0.22 μF) used in these tests.

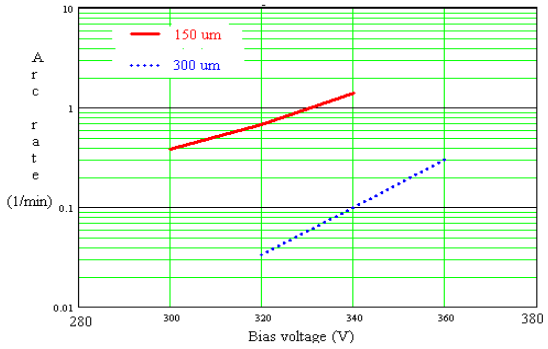

Figure 5. Arc rate on the middle strings (samples #1 and #2).

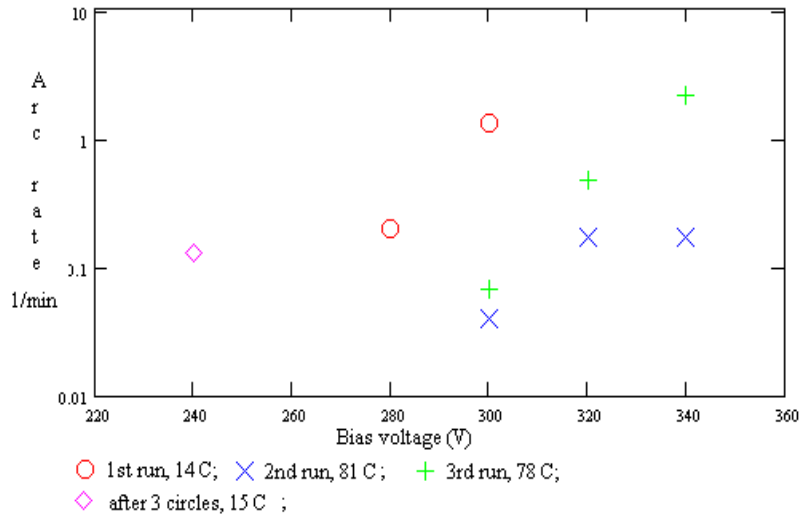

Figure 6. Arc rate on the middle string of sample #2.

To test the possibility of outgassing of the whole sample by heating it to 80 C and pumping out an excess of water vapor the sample #2 has been undergone to five thermal cycles (see Fig.4). Arc rates are measured for all three strings connected in parallel at room temperature before the first cycle and after the fifth cycle. The results are shown in Fig.7.

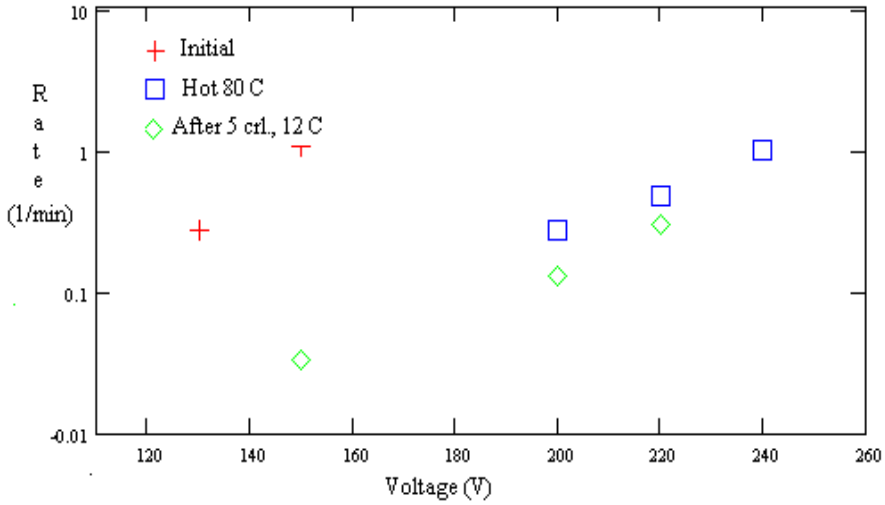

Figure 7. Arc rate on sample #2 (three strings in parallel).

It is seen in Fig.7 that arc rate decreases about 30 times and arc threshold increases approximately 30 V due to outgassing. It should be noted that minimum partial pressure of water vapor in xenon plasma reached in these experiments was 1.4 μTorr that seems not low enough to outgas sample surfaces to the degree expected in LEO.

Arcing on the sample #3 (middle string, CMX UVR coverglass) demonstrates significant increase in arc threshold (80-100 V) comparatively to arcing on sample #2. Arc inception voltage

for the middle string is 360 V, and two other strings are arcing at lower voltages due to considerable percentage of arcs on the cell edges. This observation can be explained by difference in dielectric permittivity for borosilicate and CMX glasses. Really, electric field strength in the vicinity of a triple junction is higher for dielectric with high permittivity (Fig.8). If one suggests that all other characteristics of samples #2 and #3 are identical the observed difference in arc threshold voltages can be understood. It should be noted that the conductivity of coverglass also influences the arc threshold voltage, and the direction of this effect is opposite to the previous one because of higher resistivity of CMX glass (10^{13} Ohm*m vs. 10^{12} Ohm*m for borosilicate). That may explain lower than expected from the Fig.8 observed discrepancy in arc thresholds but this problem needs more thorough investigation. The test results for the sample #4 (250 μm overhang) look also prospective. Arc inception voltage is 80-100 V higher, and arc rate is lower for the middle string. Two other strings have also demonstrated the decrease of arc rate in spite of arcing on cell edges. The increase of arc inception voltage to 480 V for the hot sample is particularly important. It seems that the array with coverglass overhang and additional insulation of cell edges can operate at 400 V in LEO conditions.

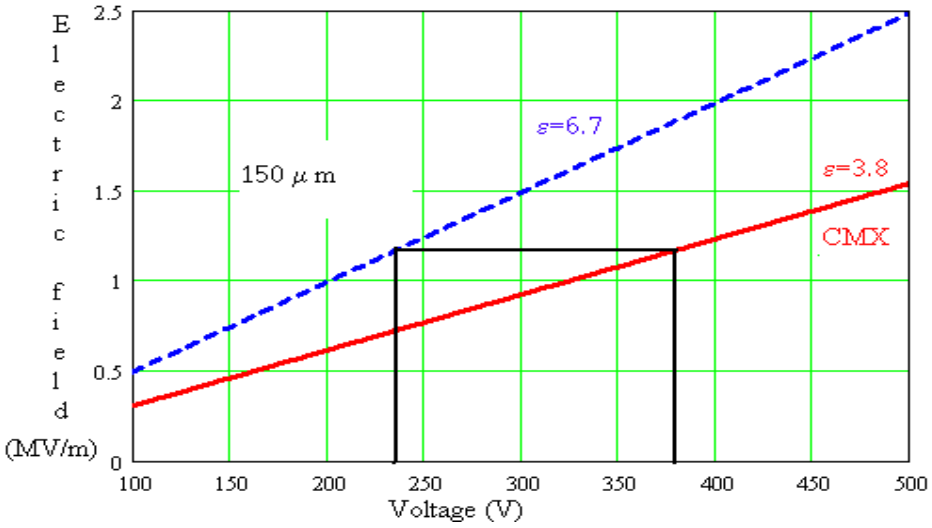

Figure 8. The difference in arc thresholds between samples with CMX and borosilicate coverglasses should be about 130 V according to the calculations of electric field strengths.

According to existing model of arc inception [12,13] the most probable arc site on an array surface is a conductor-dielectric junction exposed to the plasma. Thus, if all interconnects are insulated from the surrounding plasma the probability of a discharge decreases significantly. One of the possible realizations of this idea is the array design with wrapthrough interconnects (sample #5, Fig.9). Such design cannot prevent arcing at very high negative potential because edge of semiconductor (silicon, germanium, or other) stays exposed to the plasma, and many tests (including ones described in this paper) have demonstrated intensive arcing on cell edges. However, considerable increase of arc inception voltage can be expected, particularly for the middle string. Test results confirm these expectations (Fig.10). The inception of arc is observed on the middle string at bias voltage 440 V that is 60 V higher than arc inception voltage for the

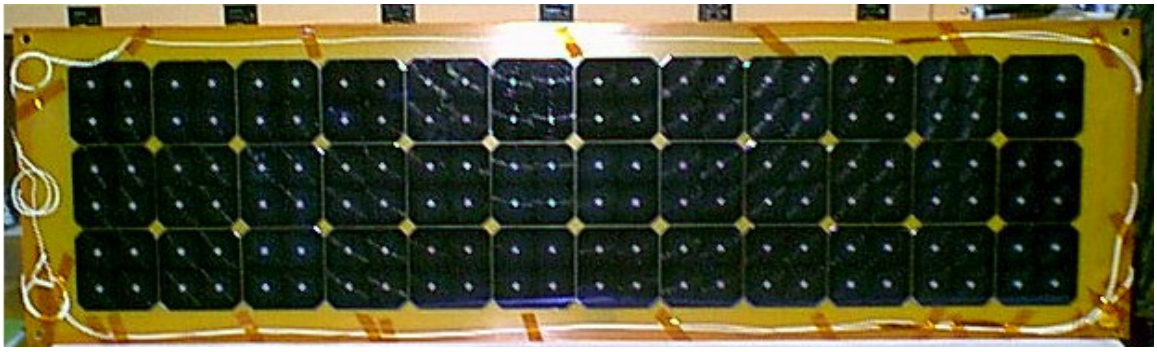

Figure 9. Solar array sample with wrapthrough interconnects.

string with coverglass overhang. Arc sites are located between adjacent cells belonging as to middle string as to neighboring strings. Two other strings demonstrate much lower arc inception voltages due to arcing on edges. Unfortunately, experimental setup has not provided a possibility to heat this sample above room temperature but even the results obtained to date show that this kind of solar array can be used in LEO to generate power at voltage 450 V if array edges are electrically insulated.

Short electrostatic discharges studied above are certainly undesirable events that must be prevented for reliable operation of the spacecraft. However, this kind of transients are not damaging solar array irreversibly, at least in cases of low additional capacitances used in current experiments. Sustained discharges initiated between adjacent cells with a few tens volt potential difference are much more dangerous [14,15] because they can destroy cells and underlying substrate that results in considerable loss of power. Samples #1, #2, and #4 have been tested against an inception of sustained arc between two strings. Test starts with lower limits on SAS voltage and current. After the registration of 5-10 arcs these parameters are gradually changed and more arcs are generated until initial sign of sustained discharge is seen on the oscilloscope. This sign represents the SAS current pulse that continues much longer than original arc. The corresponding SAS voltage and current are considered as threshold parameters because even a small increase of them (10 V and 0.25 A) results in spectacular event shown in Fig.11. In this case the sustained discharge has been quenched after 20 s by turning SAS off. Damaged part of the sample is shown in Fig.12. Threshold parameters depend on solar array design: they are 40 V and 1 A for sample #1, 60 V and 2 A for sample #2, and 80V and 1.6 A for sample #4.

Scaling of Arc Current Pulse Width and Amplitude

Even short transients are detrimental for spacecraft, and the degree of damage increases with the increase of arc current amplitude and pulse width. These two parameters depend on the amount of electrical charge leaking into surrounding plasma during the discharge time. There are currently two theoretical models that allow estimating lost electrical charge and its dependence on the array capacitance. First model [16] is based on the suggestion that the discharge generates an expanding plasma sheath neutralizing positive charge on top of coverglass. If plasma expands with a constant speed the discharge time is proportional to the array linear dimensions, or, in another terms, to the square root of an array capacitance. This dependence has been proved in many experiments [16,17]. However, the distance that plasma can expand on is limited to about

1 m in simulated LEO conditions [18]. Thus, according to the first model the upper limit for the effective capacitance is the capacitance of the part of solar array with area approximately 1 m^2.

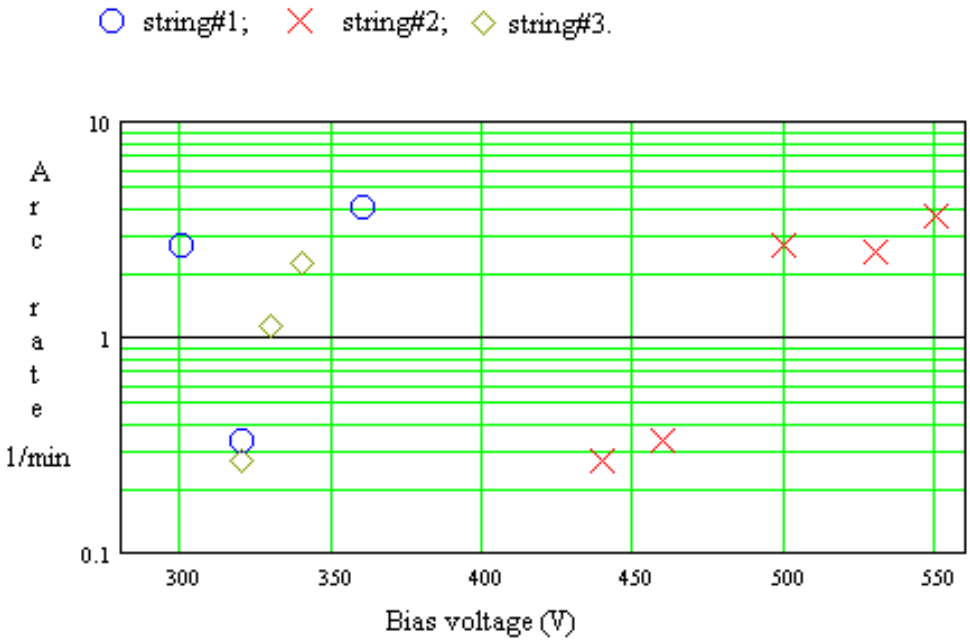

Figure 10. Arc rate on sample #5.

Figure 11. Sustained arc between adjacent strings on sample #2.

The second model also envisages that both arc current amplitude and pulse width are proportional to the square root of a capacitance but this prediction is based on the dynamics of ionization-

recombination processes in the discharge plasma [6]. If the second model is correct the effective capacitance is only two-three times less than the capacitance of a whole solar array. A simple experiment has been performed to verify the validity of the second model. Two solar array samples (sample #2) are mounted on aluminum panel with grounded aluminum plate installed between samples. The height of the plate is 7.5 cm bigger than the distance between aluminum panel and top of the sample. Such arrangement prevents the expansion of plasma sheath from one sample to another. The additional capacitor of 1000 pF is used in this particular experiment.

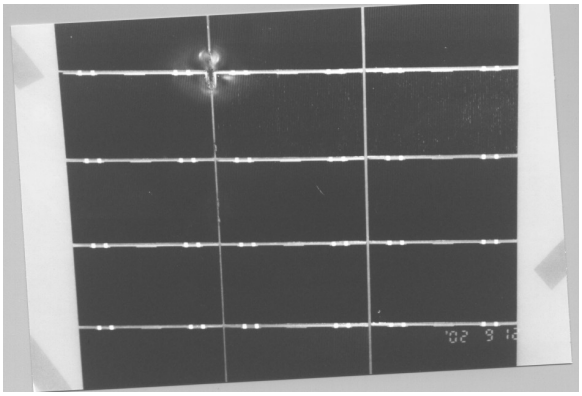

Figure 12. Damage induced by sustained arc.

The capacitance of one cell can be calculated as

$$C_1 = \frac{\varepsilon_0 \varepsilon_1 S_1}{d_1}\left(1+\frac{\varepsilon_1 d_2}{\varepsilon_2 d_1}\right)^{-1} \qquad (1)$$

where $\varepsilon_{1,2}$ are dielectric constants of coverglass and adhesive, $d_{1,2}$ are their thicknesses, and S_1 is a cell area.

Dielectric constants are: for borosilicate coverglass ε_1=6.7, and for epoxy ε_2=3.6. Thus, a quite reliable estimate can be obtained: C_1=590 pF/cell. Moreover, the scaling does not practically depend on exact numbers for largest capacitances. Ten measurements of arc current pulse widths for each configuration have been done by biasing one string, three strings, and six strings in parallel. The results are shown in Fig.13. The scaling is confirmed with a very high accuracy, which means that adequate ground simulations of arcing on spacecraft surfaces have to be performed with a very large additional capacitance (for instance, about 1000 μF for ISS).

Current Collection

One solar cell provides current of 1 A in order of magnitude while collected current is scaled in hundred micro amps. Thus, the role of collected current in a parasitic power drain is certainly negligible. However, the floating potential of the spacecraft strongly depends on the current collected by the solar array [19]. There are three main factors that influence the magnitude of collected current: I) solar array design; II) solar array temperature; III) parameters of surrounding

plasma. Obviously, the design with coverglass overhang and with wrapthrough interconnects offers arrays with considerably decreased collected currents. Electron number density and electron temperature also influence on current collection. Ground tests that simulate an electron component of LEO plasma quite reasonably provide reliable data for current collection by cells with positive potentials with respect to surrounding plasma. Test data containing measurements of collected current for negatively biased cells are applicable to the analysis of spacecraft floating potential not better than in order of magnitude because the characteristics of ion component are different in ground tests and in LEO.

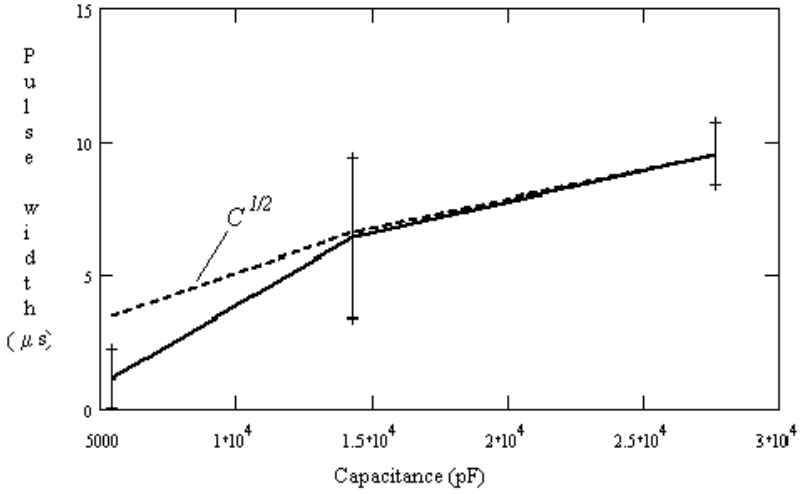

Figure 13. Pulse width scaling measured by biasing to -340 V one, three, and six strings of sample #2. Error bars (±1σ) are calculated from ten measurements for each point.

A few examples of the dependence of electron current collection on bias voltage are shown in Fig.14. It is seen than the increase of electron number density results in the almost proportional increase in current collection. But the dominant factor in the current collection is an array temperature. The magnitude of collected current grows more than three times when array temperature reaches 79 C. This observation must be taken into account for the computations of spacecraft floating potentials. Ion currents are measured by biasing separate strings up to 100 V negative, and these currents do not exceed 1 μA for all situations studied even though the same effect of significant increase due to heating is also found.

Measurements of collected currents for the sample with coverglass overhang have demonstrated the decrease in magnitude close to the factor 2 comparatively to sample with a standard design. Cell with wrapthrough interconnects collects not much less current than cell with coverglass overhang but it generates three times higher power. It seems that tests in simulated plasma environment are suitable for creation a data base for further computations of the spacecraft floating potentials in LEO.

Conclusions

Comprehensive tests of five different types of solar array samples in simulated LEO plasma environment have demonstrated that the highest arc threshold (440 V) can be achieved for an array with wrapthrough interconnects if edges of strings are not exposed to the plasma. This design is also effective in decreasing of an array current collection. The design with exposed interconnects but with coverglass overhang also provides significant improvement comparatively to the conventional design. Particularly, arcing on the sample cannot be initiated at potentials below 300 V even under room temperature, and arc threshold increases to 420 V under temperature 72 C. The increase of coverglass thickness also results in some improving of array parameters. Thorough outgassing of solar array surfaces may result in significant decrease of arc rate for a conventionally designed solar array.

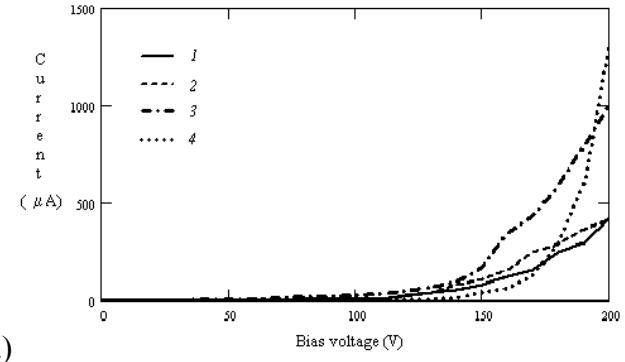

a)

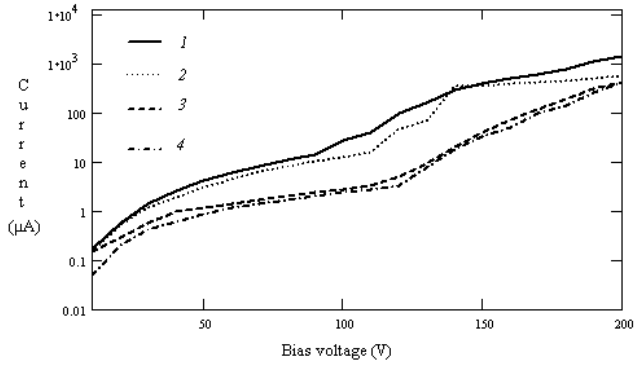

b)

Figure 14. Electron current collection:

a) *1*-sample #2, str.2, n_e=2*10^5 cm^{-3},15 C; *2*-sample #1, str.1, n_e=7*10^5 cm^{-3},15 C; *3*-sample #1, str.2, n_e=2*10^6 cm^{-3},15 C; *4*-sample #2, str.1, n_e=5*10^5 cm^{-3}, 79 C.

b) b)*1*-sample #3, str.2, n_e=1*10^6 cm^{-3}; *2*- sample #4, str.2, n_e=1*10^6 cm^{-3}; *3* and *4*-sample #5, str.1 and 2 respectively, n_e=3.5*10^5 cm^{-3}, temp. 15 C.

References

(1) Stevens, N.J. "Interactions Between Spacecraft and the Charge-Particle Environment", Proc. Spacecraft Charging Technology Conference, NASA CP-2071, 1978, p.268-294.

(2) Ferguson, D.C. "Solar Array Arcing in Plasmas", NASA CP-3059, 1989, p. 509.

(3) Hastings, D.E. "A Review of Plasma Interactions With Spacecraft in Low Earth Orbit", Journal of Geophys. Research, Vol.100, No.A8, 1995, pp.14,457-14,483.

(4) Parks, E.D., Jongeward, G., Katz, I., and Davis, V.A. "Threshold-Determing Mechanisms for Discharges in High Voltage Solar Arrays", Journal of Spacecraft and Rockets, Vol.24, No.4, 1987, pp.367-371.

(5) Upschulte, B.L., Marinelli, W.J., Carleton, K.L., Weyl, G., Aifer, E., and Hastings, D.E. "Arcing on Negatively Biased Solar Cells in a Plasma Environment", Journal of Spacecraft and Rockets, Vol.31, No.3, 1994, pp.493-501.

(6) Vayner, B., Galofaro, J., Ferguson, D., and Degroot, W. "Electrostatic Discharge Inception on a High-Voltage Solar Array", AIAA Paper 2002-0631, Jan.2002.

(7) Galofaro, J., Vayner, B., Ferguson, D., and Degroot, W. "A Desorbed Gas Molecular Ionization Mechanism for Arcing Onset in Solar Arrays Immersed in a Low-Density Plasma", AIAA Paper 2002-2262, May 2002.

(8) Anders, A., and Anders, S. "Emission Spectroscopy of Low-Current Vacuum Arcs", Journal of Physics D: Appl. Phys., Vol.24, 1991, pp.1986-1992.

(9) Yotsombat, B., Davydov, S., Poolcharuansin, P., Vilaithong, T., and Brown, I.G. "Optical Emission Spectra of a Copper Plasma Produced by a Metal Vapor Vacuum Arc Plasma Source", Journal of Physics D: Appl. Phys., Vol.34, 2001, pp.1928-1932.

(10) Pearse, R.W.B., and Gaydon, A.G. "The Identification of Molecular Spectra", 3rd edition, Chapman & Hall LTD, London, UK, 1963, 347p.

(11) Vayner, B.V., Galofaro, J.T., and Ferguson, D.C. "The Neutral Gas Desorption and Breakdown on a Metal-Dielectric Junction Immersed in a Plasma", AIAA Paper 2002-2244, May 2002

(12) Cho, M., and Hastings, D.E. "Computer Particle Simulation on High-Voltage Solar Array Arcing Onset", Journal of Spacecraft and Rockets, Vol.30, No.2, 1993, pp.189-205.

(13) Hastings, D.E., Weyl, G., and Kaufman, D. "Threshold Voltage for Arcing on Negatively Biased Solar Arrays", Journal of Spacecraft and Rockets, Vol.27, No.5, 1990, p.539-544.

(14) Hoeber, C.F., Robertson, E.A., Katz, I., Davis, V.A., and Snyder, D.B. "Solar Array Augmented Electrostatic Discharge in GEO", AIAA Paper 98-1401, Jan. 1998.

(15) Snyder, D.B., Ferguson, D.C., Vayner, B.V., and Galofaro, J.T." New Spacecraft-Charging Solar Array Failure Mechanism" 6th Spacecraft Charging Technology Conference, Nov. 2-6, 1998, Air Force Res. Lab., Hanscom AFB, MA, USA, pp.297-301.

(16) Balmain, K. G., and Dubois, G. R. "Surface Discharges on Teflon, Mylar and Kapton," IEEE Transactions on Nuclear Science, Vol. 26, No.12, 1979, pp.5146-5151.

(17) Snyder, D.B. "Characteristics of Arc Currents on a Solar Cell Array in a Plasma", IEEE Transactions on Nuclear Science, Vol.31, No.4, 1984, pp.1584-1587.

(18) Cho, M., Ramasamy, R., Hikita, M., Tanaka, K., and Sasaki, S. "Plasma Response to Arcing in Ionospheric Plasma Environment: Laboratory Experiments", Journal of Spacecraft and Rockets, Vol.39, No.3, 2002, pp.392-408.

(19) Ferguson, D.C., and Hillard, G.B. "In-Space Measurements of Electron Curren Collection by Space Station Solar Arrays", AIAA Paper 95-0486, Jan. 1995.